

# VIBROACOUSTIC SIMULATION OF HETEROGENEOUS MULTILAYER COMPOSITE PLATES INVOLVING LOW YOUNG'S MODULUS VISCOELASTIC MATERIALS

## A. CASTEL - DRIVE

A. LOREDO - A. EL HAFIDI - S. TORRES MAÑUECO - DRIVE

DRIVE, Universite de Bourgogne, 49 rue Mlle Bourgeois, 58027 Nevers, France

### Abstract

The vibroacoustic behavior of composite multilayered plates involving high Young's modulus ratios between adjacent layers, like sandwich panels and passive constrained layer damped plates, is studied. As classical plate models give poor results with such structures, a specific model has been used. It is an *equivalent single layer* model, with a five unknown displacement field which takes into account a variation of transverse shear strains into the thickness. A classical sandwich structure is simulated, its natural frequencies are compared to those given by other models and a 3D finite element simulation which is taken as reference. A second study concerns a composite plate with a damping patch in which the constraining layer is a unidirectional ply. Comparisons for two orientations of this ply (0° or 90°) are presented.

## 1 INTRODUCTION

In plate structures, it is common to combine different materials with very different Young's moduli and densities. Two interesting applications are sandwich structures, where the core materials (e.g., foam, honeycomb) usually have a low density and a low stiffness compared to the skins, and passive damping patches where a thin layer of high loss factor viscoelastic material is applied. In both cases, the Youngs modulus ratio of two adjacent layers can reach  $10^5$ . Classical plate theories usually give poor results with such a high Young's modulus ratio; therefore, a more advanced plate model is required. In this work, an anisotropic multilayer plate model with a particular displacement field, originally developed by Sun & Whitney [1], is used; it defines the displacement of all the layers of the panel as a function of the displacement of the first layer using the assumptions of continuity of displacements and transverse shear stresses at the interfaces between layers. The central role played by the base layer makes the model perfectly adapted to the study of damping patches, which do not classically cover the entire structure. In addition, the displacement field is particularly adapted to highly inhomogeneous plates, which also includes classical sandwich structures. Based on this plate theory, a discrete vibroacoustic model has been developed using the Rayleigh-Ritz method [2], in order to simulate the behavior of composite plates damped with passive constrained layer patches. The model solves the complex

system of laminate equations of motion under harmonic excitation. It can manage different loadings: concentrated forces, acoustic plane wave and diffuse field. It can compute complex displacements, strains, and stresses in each layer. In addition, it outputs the usual vibroacoustic indicators (e.g., mean square velocity, transmission loss, radiated power) for the studied panels. Two studies are presented:

- a – Computation of the natural frequencies is performed for an antisymmetric composite sandwich structure [0°/90°/core/0°/90°] from the literature [3]. Results are compared with those of classical plate models, three dimensionnal finite element calculations and the literature.
- b – A composite plate made of eight plies [0°/45°/90°/-45°]S covered over 40% of its surface with a constrained layer damping patch is studied. The constraining layer is made of a single unidirectional ply (two orientations are tested). Results are presented in terms of mean quadratic velocity.

## 2 PRESENT PLATE MODEL

The present model has been presented in reference [2]. It permits to simulate the behavior of a rectangular multilayered plate with one or several multilayered patches. It is based on a displacement field obtained by means of kinematic and static considerations. This approach was used in the early work of Sun & Whitney [1] for multilayered plates and has been used later for vibroacoustical purposes by Guyader and Lesueur [4].

It is a two-dimensional plate model with the five classical displacement unknowns, but it differs from classical laminate theories (CLT) and shear deformation theory (SDT) since the assumed displacement variation, with respect to  $z$ , is piecewise linear. This is the result of writing continuities of both displacements and shear stresses at each interface, as shown below. For practical reasons, the displacement field of each layer  $\ell \in [2..n]$  is linked to the displacement field of the first layer. Thicknesses and elevations for an  $n$  layer material are presented in figure 1. The displacement field in each layer is written as follows,

$$\begin{cases} u_\alpha^\ell(x, y, z) &= u_\alpha^\ell(x, y, z^\ell) + (z^\ell - z)(u_{3,\alpha}^1(x, y) - \gamma_{\alpha 3}^\ell(x, y)) \\ u_3^\ell(x, y, z) &= u_3^1(x, y) \end{cases} \quad (1)$$

where greek indices stand for in-plane quantities and take values 1 or 2, superscript  $\ell$  stands for the  $\ell$ -th layer and superscript 1 stands for the first layer for which all will be related,  $\gamma_{\alpha 3}^\ell(x, y)$  are the transverse (engineering) shear strains, and  $z^\ell$  is the elevation of the layer  $\ell$ .

With these assumptions, the transverse displacement  $u_3$  and the transverse shear strains  $\gamma_{\alpha 3}^\ell$  are constant within each layer with respect to the  $z$ -coordinate. Therefore, transverse shear stresses will also be constant in each layer. According to these remarks, the previously mentioned continuities of displacements and shear stresses reduce to:

$$\begin{cases} u_\alpha^\ell(x, y, z^\ell + h^\ell/2) &= u_\alpha^{\ell+1}(x, y, z^{\ell+1} - h^{\ell+1}/2) \\ \sigma_{\alpha 3}^\ell(x, y) &= \sigma_{\alpha 3}^{\ell+1}(x, y) \end{cases} \quad (2)$$

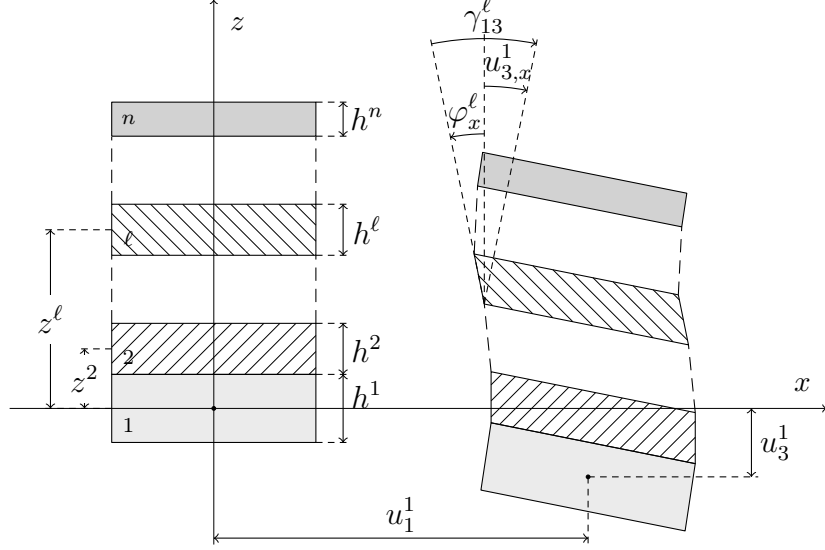


Figure 1: Geometrical parameters of the multilayer structure (represented on the left side in an undeformed state) and displacements (represented on the right side after deformation).

Equation (2) allows to link the displacement field in the  $(\ell + 1)$ -th layer with the one of the  $\ell$ -th layer, and, recursively, it can be linked to the displacement field of the first layer, following a process detailed in reference [4].

For patched structures, the first layer is common to the uncovered and covered parts of the plate, therefore all the displacements in the multilayered structure are known in terms of the first layer's displacement field, including only the five classical plate unknowns: three displacements  $u_i^1$  and two rotations  $\varphi_\alpha^1 = u_{3,\alpha}^1 - \gamma_{\alpha 3}^1$ .

However, this plate model can be set into the refined shear theories family as it was shown in reference [5]. The kinetic and static assumptions of equation (2) permit to formulate four warping functions that can be used to define the displacement field in a classical manner. Hence, the laminate static behavior involves 55 generalized stiffness constants (a  $10 \times 10$  and a  $2 \times 2$  matrix) linking the 12 generalized displacements (3 membrane strains  $\varepsilon_{\alpha\beta}$ , 3 bending curvatures  $\kappa_{\alpha\beta} = -w_{,\alpha\beta}$ , 4 transverse shear strain derivatives  $\Gamma_{\alpha\beta} = \gamma_{\alpha 3,\beta}$ , and 2 shear strains  $\gamma_{\alpha 3}$ ) to the 12 corresponding generalized forces ( $N_{\alpha\beta}$ ,  $M_{\alpha\beta}$ ,  $P_{\alpha\beta}$  and  $Q_\alpha$ ) :

$$\begin{Bmatrix} \mathbf{N} \\ \mathbf{M} \\ \mathbf{P} \end{Bmatrix} = \begin{bmatrix} \mathbf{A} & \mathbf{B} & \mathbf{E} \\ \mathbf{B} & \mathbf{D} & \mathbf{F} \\ \mathbf{E}^T & \mathbf{F}^T & \mathbf{G} \end{bmatrix} \begin{Bmatrix} \boldsymbol{\varepsilon} \\ \boldsymbol{\kappa} \\ \boldsymbol{\Gamma} \end{Bmatrix} \quad \{\mathbf{Q}\} = [\mathbf{H}] \{\boldsymbol{\gamma}\} \quad (3)$$

Concerning the dynamic behavior, the kinetic energy involves 18 generalized mass terms acting on the 7 generalized speeds (2 in-plane speed  $\dot{u}_\alpha$ , 1 transverse speed  $\dot{w}$ , 2 bending speeds  $-\dot{w}_{,\alpha}$  and 2 transverse shear speeds  $\dot{\gamma}_{\alpha 3}$ ). The complete development of the laminate motion equations can be found in the aforementioned reference.

The construction of the discrete motion equation system is achieved by the Rayleigh-Ritz method. Various boundary conditions and external solicitations can be considered, as it is presented in detail in reference [2]. In this reference, the vibroacoustic indicators computation from the outputs of the dynamic model is also detailed. However, this model uses at this time the enriched trigonometric basis described in [6] instead of the trigonometric basis presented in reference [2], this last one has been found to be unstable when order higher than 15 were used.

In addition, a post-processing toolbox that permits to compute the local complex power in the laminate has been developed. It is presented in reference [7]. It has been found to be a powerful tool to understand the damping behavior of such heterogeneous structures. These post-processing units permit to compute the incoming complex power, the dissipated power and the conservative powers (kinetic and strain contributions). These computations can be performed locally (*i.e.* for  $(x, y, z)$ ), or for a surface location (*i.e.* for  $(x, y)$ , summation on  $z$ ) that permits to plot maps, or for a single layer to separate the different material contributions, or for the entire structure. In addition, it is possible to separate the tensors components contributions to each quantity. Ratios between some of these quantities are meaningful and can be used to quantify and to optimize the damping.

### 3 ANTISYMMETRIC COMPOSITE SANDWICH STRUCTURE

This section aims at studying a five layer sandwich plate  $[0^\circ/90^\circ/\text{core}/0^\circ/90^\circ]$  with a fixed ratio of thickness core to flange  $t_c/t_f = 10$ . The face sheets (Graphite-Epoxy T300/934) have the following properties:

$$E_1^f = 131 \text{ GPa}, E_2^f = 10.34 \text{ GPa}, E_2^f = E_3^f, G_{12} = 6.895 \text{ GPa}, G_{13}^f = 6.205 \text{ GPa}, G_{23}^f = 6.895 \text{ GPa}, \nu_{12}^f = \nu_{13}^f = 0.22, f u_{23} = 0.49, \rho^f = 1627 \text{ kg.m}^{-3}.$$

The core material is made of an isotropic foam with the following properties:

$$E_1^c = E_2^c = E_3^c = 6.89 \times 10^{-3} \text{ GPa}, G_{12}^c = G_{13}^c = G_{23}^c = 3.45 \times 10^{-3} \text{ GPa}, \nu_{12}^c = \nu_{13}^c = \nu_{23}^c = 0, \rho^c = 97 \text{ kg.m}^{-3}$$

Six natural frequencies obtained with six different models are compared:

- the present model – 5 displacements variables,
- the classical Mindlin-Reissner plate model with shear correction factors set to 0.003186 (M-R SCF) – 5 displacements variables,
- the classical Mindlin-Reissner (M-R) plate model – 5 displacements variables,
- the 3D finite element formulation which is supposed to be exact –  $[(2 \times N + 1) \times 3]$  displacements variables for  $N$  elements over the thickness,
- the layer wise (LW) model of Rao [8] –  $[(N + 1) \times 6]$  displacements variables for  $N$  layers,
- the equivalent single layer (ESL) model of Rao [8] – 12 displacements variables.

$m$	$n$	Present model	MR with SCF	MR	HDST	3D FEM	Rao (LW) [8]	Rao (ESL) [8]
$a/H = 10$								
1	1	1.8481	1.7438	13.8515	7.1342	1.8480	1.8480	4.9624
1	2	3.2232	2.7679	31.9890	12.1471	3.2204	3.2796	8.1934
1	3	5.2362	3.9208	55.8118	17.7164	5.2279	5.2234	11.9867
2	2	4.2904	3.5043	43.4895	15.6322	4.2911	4.2894	10.5172
2	3	6.0973	4.4709	62.3564	20.2753	6.0993	6.0942	13.7488
3	3	7.6712	5.2627	76.8282	24.0646	7.6849	7.6762	16.4514
$a/H = 100$								
1	1	11.6333	11.7177	16.2799	15.6790	11.9457	11.9401	15.5480
1	2	23.1617	23.1913	44.5302	41.9435	23.4031	23.4017	39.2652
1	3	36.0222	35.9085	95.0282	84.0773	36.1430	36.1434	73.4951
2	2	30.6842	30.7059	63.8371	59.3859	30.9430	30.9432	55.1512
2	3	41.2521	41.1568	108.2557	95.7435	41.4470	41.4475	84.2919
3	3	49.6040	49.4154	142.6021	123.4348	48.9995	49.7622	106.5897

Table 1: Variation of nondimensionalized fundamental frequencies  $\bar{\omega} = (\omega a^2/h) \sqrt{\rho^f/E_2^f}$  for a composite sandwich panel with  $L/h$  varying and  $t_c/t_f = 10$

Table 1 shows that the present model is the most accurate of the equivalent single layer models. Note that models in which displacements variables over the thickness depends on the number of layers (or the number of elements) show a good accuracy but those models are not as efficient in term of computation performance. It has been shown in [5] that the present model shows a very good agreement when the Young's modulus ratio between the layers is quite high (over  $10^4$ ).

Results obtained with the MR with SCF model and the present model are acceptable for the second panel but still not as accurate as the LW model from Rao. This can be explained since the present model is not the most appropriate for thin structures.

## 4 PATCHED COMPOSITE PLATE

This section aims at studying the mechanical and acoustical behavior of a composite square plate  $[0^\circ/45^\circ/90^\circ/-45^\circ]_S$  with a side length of  $L = 1$  m and clamped boundary conditions. Every ply is made of 0.15 mm of Graphite-Epoxy T300/934 (material properties are given in section 3, damping factor of the composite is arbitrarily set to  $\eta = 0.0016$ ). The structure is excited by a plane wave traveling towards the plate with incidence angles  $\theta = 45^\circ$ ,  $\varphi = 45^\circ$ , and amplitude 1 Pa (see figure 2 for corresponding definitions).

Three cases are studied:

- The naked plate without any damping patch,
- The plate covered on 40% of its surface with a damping patch made of 0.15 mm of ISD112 and one 0.15 mm ply of Graphite-Epoxy T300/934 at  $0^\circ$ ,
- The plate covered on 40% of its surface with a damping patch made of 0.15 mm of ISD112 and one 0.15 mm ply of Graphite-Epoxy T300/934 at  $90^\circ$ .

The ISD112 properties are frequency dependent and detailed in table 2.

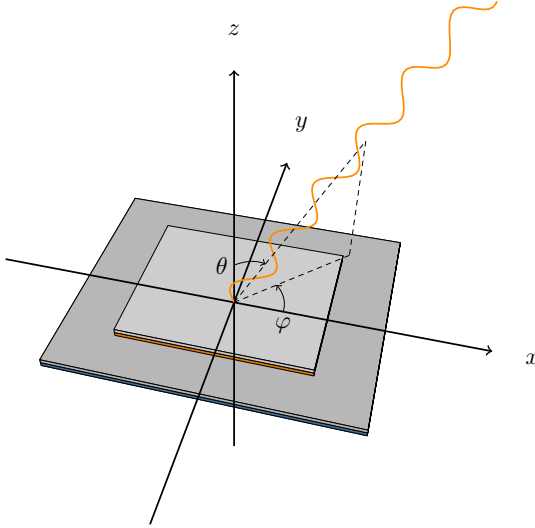


Figure 2: View of a patched plate submitted to an acoustic plane-wave, showing the definition of the angles of incidence  $\theta$  and  $\varphi$ .

Frequency (Hz)	Young's Modulus (Pa)	Loss factor $\eta$
10	$7.28 \times 10^5$	0.90
100	$2.34 \times 10^6$	1.00
500	$5.20 \times 10^6$	1.00
1000	$7.28 \times 10^6$	0.90
2000	$9.88 \times 10^6$	0.80
3000	$1.17 \times 10^7$	0.75
4000	$1.38 \times 10^7$	0.70

Table 2: Frequency dependence of the mechanical properties of the viscoelastic material ISD 112 ( $T = 25^\circ$ )

Figure 3(a) shows the plates' mean square velocity up to 3 kHz. It is clear that the patch has limiting effect on the mean square velocity over the plate. Note that the orientation of the ply of the constraining layer has an influence.

The study is now focusing on two frequencies for which a typical behavior is observed. The first frequency is 87 Hz, mean square velocity versus frequency is detailed around that frequency on figure 3(a), we can see that the two patches have a different efficiency at this frequency. Figure 4 shows the displacement and the mean square velocity for both patched configurations. We can see on figure 4(a) that the  $0^\circ$  constraining layer ply let a  $1 \times 5$  mode appear when on figure 4(b) this same mode is not appearing and therefore mean square velocity is about ten times lower.

The second considered frequency is 2375 Hz. At this frequency, we can see on figure 3(c) that the patch does not damp the structure very well. When looking at the mean square velocity maps presented in figure 5 we can see that the patch does damp where it is located, but mean square velocity all around the patch is quite high and therefore we can say this patch layout is not appropriate for higher frequencies mode shape. In order to evaluate the damping efficiency of the patches several energetic

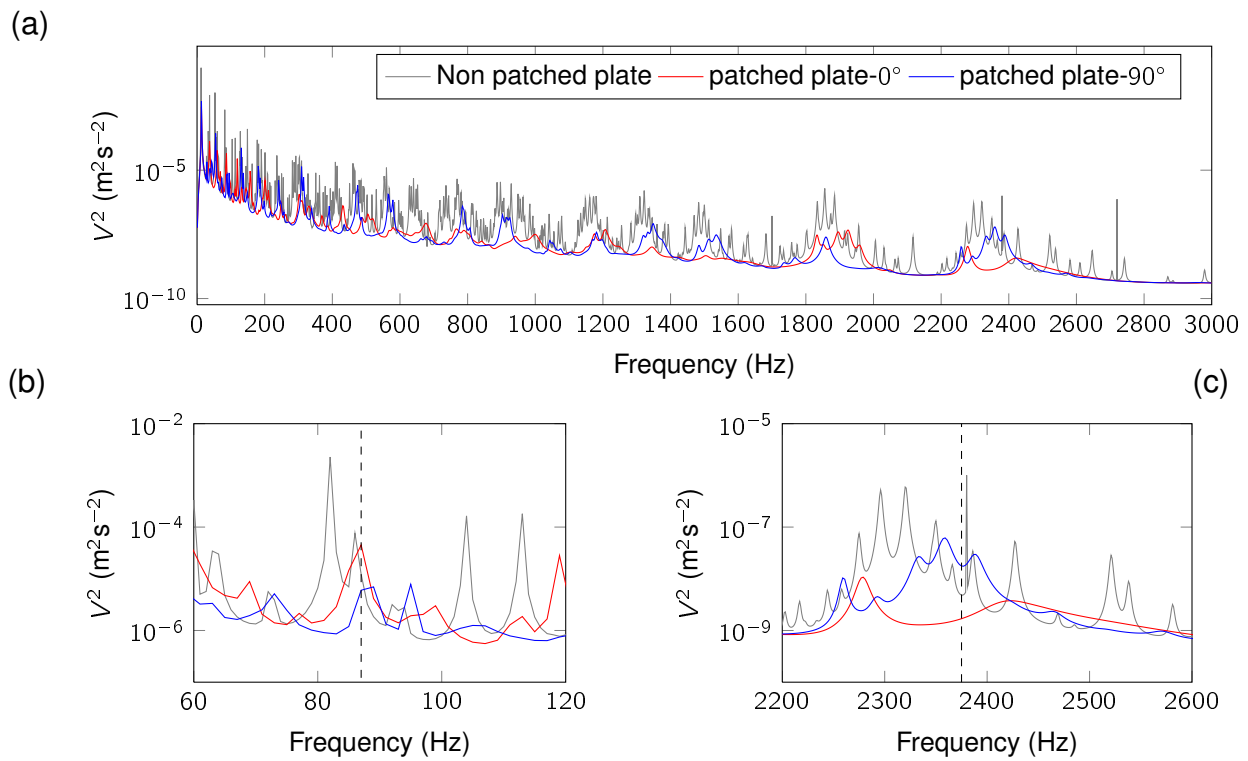


Figure 3: Mean Square Velocity versus frequency for the three studied structures. (a) Mean square velocity over the 0 - 3000 Hz range. (b) First focus point : 87 Hz. (c) First focus point : 2375 Hz.

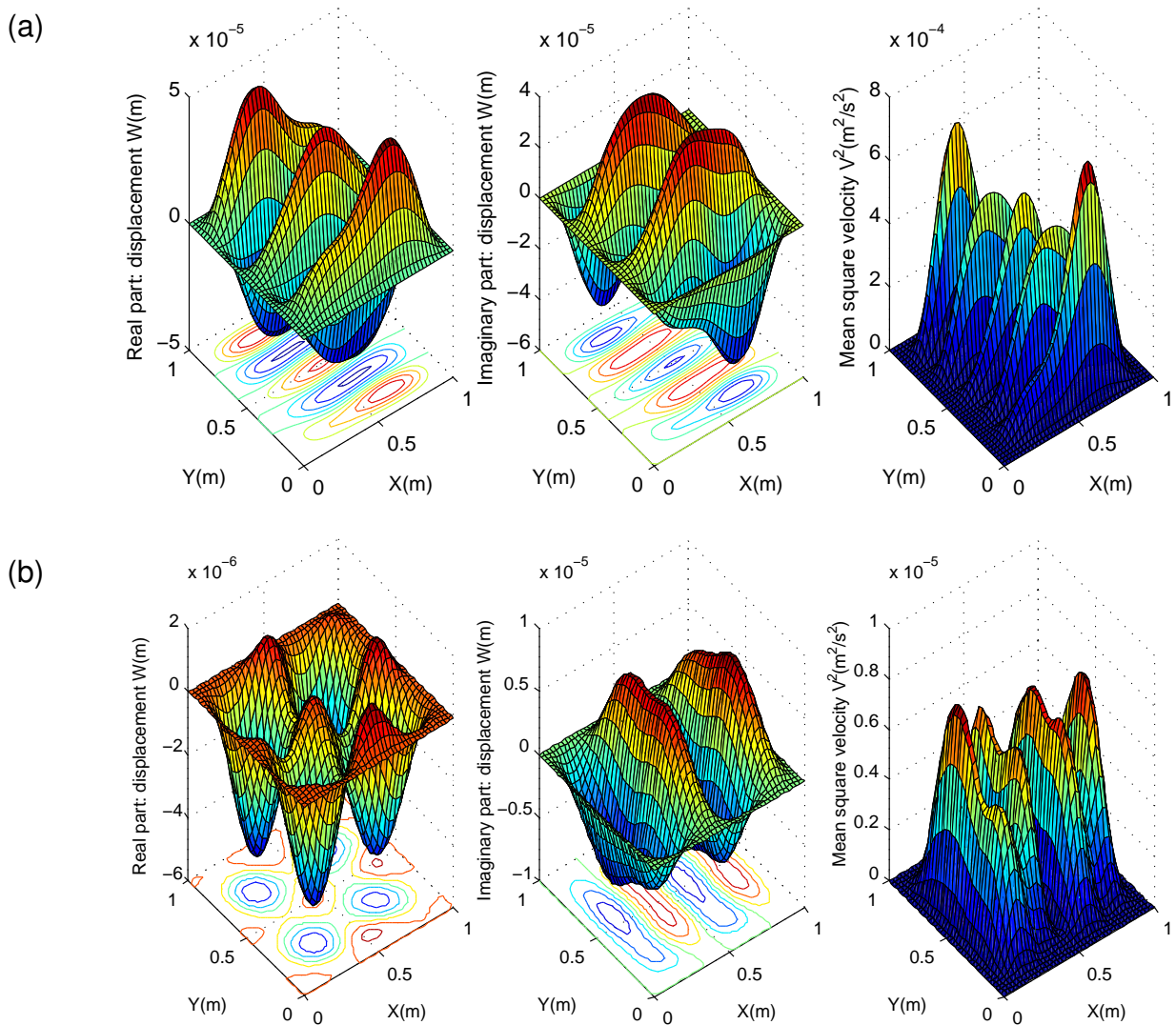


Figure 4: Mean square velocity, real and imaginary displacements for (a) the  $0^\circ$  constraining layer ply and (b) the  $90^\circ$  constraining layer ply.

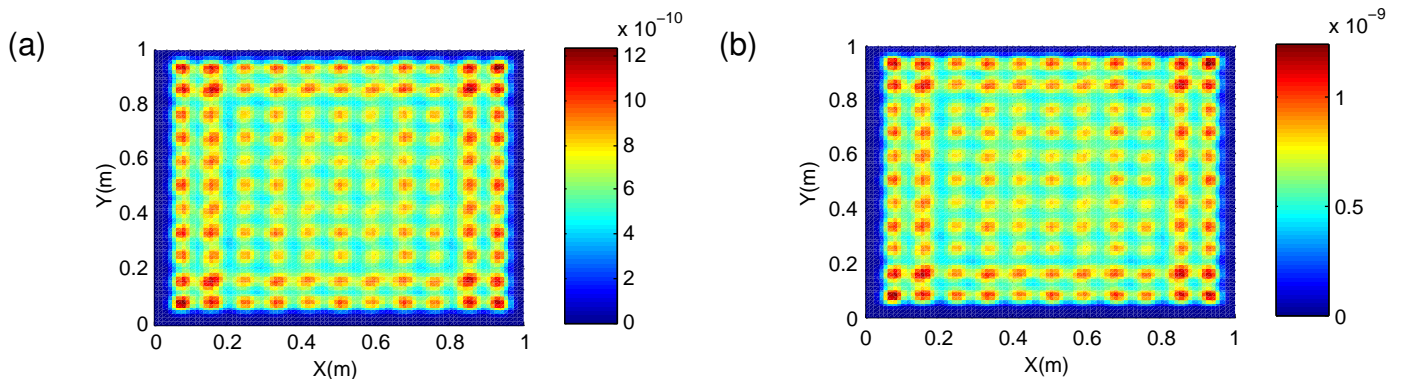


Figure 5: Mean square velocity at 2375 Hz for (a) the  $0^\circ$  constraining layer ply and (b) the  $90^\circ$  constraining layer ply.

criteria, proposed in [7], could be used to improve the patches layout and avoid this kind of behavior.

## 5 CONCLUSION

A Rayleigh-Ritz-based code which implements a specific anisotropic plate model has been used to simulate the vibroacoustic behavior of structures having high Young's modulus ratios between adjacent layers. Such structures are common nowadays in many industrial domains, including transports. Sandwich structures and patch-damped plates are two examples of practical interest.

The particularity of the considered plate model is that, although it is an *equivalent-single-layer* model with only a five-unknown displacement field, takes into account an out-of plane variation of the transverse shear strains by means of kinematic and static assumptions. The model assumes the transverse shear stresses as constant over  $z$  and hence, is not suitable for the study of homogeneous plates without the help of shear correction factors (for the single layer case, the present model is equivalent to the Mindlin-Reissner model). On the contrary, this model is particularly efficient when multilayered plates with high Young's modulus ratio between layers are simulated. It has been shown in previous papers [7, 5] that results very close to those of 3D finite element simulations can be computed with a much lower computational cost.

In this paper, additional results involving composite structures have been computed. A classical sandwich structure is simulated in terms of natural frequencies and the results are compared to other models, taken from literature or computed for the occasion, and to a 3D finite element simulation which is taken as reference. Another study concerns a passive constrained layer damped plate. To illustrate the behavior of the model, the considered constrained layer has been taken as a single unidirectional composite ply with orientation set to  $0^\circ$  or  $90^\circ$ . Comparisons of these two configurations are presented in terms of mean square velocity and also in terms of deformed shapes for some particular frequencies.

## ACKNOWLEDGMENT

This work was supported by the *Burgundy Region* and the *European Regional Development Fund*.

## References

- [1] C.T. Sun and J.M. Whitney. Theories for the dynamic response of laminated plates. *American Institute of Aeronautics and Astronautics Journal*, 11:178–183, 1973.
- [2] A. Loredo, A. Plessy, A. El Hafidi, and N. Hamzaoui. Numerical vibroacoustic analysis of plates with constrained-layer damping patches. *The Journal of the Acoustical Society of America*, 129(4):1905–1918, 2011.

- [3] T. Kant and K. Swaminathan. Analytical solutions for free vibration of laminated composite and sandwich plates based on a higher-order refined theory. *Composite Structures*, 53(1):73 – 85, 2001.
- [4] J.L. Guyader and C. Lesueur. Acoustic transmission through orthotropic multilayered plates, part i :plate vibration modes. *Journal of Sound and Vibration*, 97:51– 68, 1978.
- [5] A. Loredo and A. Castel. A multilayer anisotropic plate model with warping functions for the study of vibrations reformulated from Woodcock's work. February 2012.
- [6] O. Beslin and J. Nicolas. A hierarchical functions set for predicting very high order plate bending modes with any boundary conditions. *Journal of Sound and Vibration*, 202(5):633 – 655, 1997.
- [7] A. Castel, A. Loredo, A. El Hafidi, and B. Martin. Complex power distribution analysis in plates covered with passive constrained layer damping patches. *Journal of Sound and Vibration*, 331(11):2485 – 2498, 2012.
- [8] M.K. Rao and Y.M. Desai. Analytical solutions for vibrations of laminated and sandwich plates using mixed theory. *Composite Structures*, 63(3-4):361 – 373, 2004.